Polarization of Tensor Mesons in ψ Radiative Decays and Possible Implications for the Gluonic Content of the $\theta(1720)$

F. E. Close[(1),(2),(3)] and Z. P. Li[(1)]

[(1)]*Department of Physics, University of Tennessee, Knoxville, Tennessee 37996-1200*
[(2)]*Physics Division, Oak Ridge National Laboratory, Oak Ridge, Tennessee 37831-6373*
[(3)]*Theory Division, Rutherford Appleton Laboratory, Chilton, Didcot, Oxon, OX11 0QX, England*
(Received 17 December 1990)

We present a resolution to the problem of the helicity structure of tensor mesons produced in $\psi \to \gamma T$. The new feature is that the diagrams are separated according to their different topologies, the corresponding helicity structures being analyzed for each diagram. Different topologies appear to dominate the $f_2(1270,1525)$ $q\bar{q}$ production and the $\theta/f_2(1720)$ production, suggesting that the θ production samples large transverse momentum p_t in the ψ wave function.

PACS numbers: 13.40.Hq, 12.38.Bx, 13.88.+e, 14.40.Cs

According to quantum chromodynamics, the production of light mesons X in the radiative decay of the psi, $\psi \to \gamma X$, proceeds by the sequence $\psi \to \gamma gg \to \gamma X$. This presence of a gluonic intermediate state has caused this channel to be a favorite for seekers of gluonic hadrons —a strategy that is reinforced by the discovery of mesons, such as $\eta(1440)$ and $\theta/f_2(1720)$, that had not been seen prominently in hadronic processes. Recent advances in identifying the $q\bar{q}$ nonets in the 1-2-GeV region,[1] including the scalar mesons near the $K\bar{K}$ threshold,[2] now give hope that the low-lying glueballs ($J^{PC}=0^{++},2^{++},0^{-+}$) and hybrids may become more readily identified.[3] In this regard $\psi \to \gamma X$ becomes of significant interest.

If we are to identify gluonic hadrons, spectroscopy alone is unlikely to be sufficient: Ways of probing their constitution will be needed. One attack would be to make clear predictions about the production characteristics (such as rates, angular distributions, or helicity amplitudes) of gluonic states in $\psi \to \gamma X$, enabling one to distinguish them from $X=q\bar{q}$. However, this aim is presently stalled due, in part, to the emerging evidence that the QCD applications to $\psi \to \gamma X$ are incomplete. For example, we note the following: (a) Lattice QCD and models uniformly agree that the lightest glueballs are 0^{++}; yet no clear resonance state is seen in $\psi \to \gamma 0^{++}$. (b) The (oft-used) approximation that the intermediate gluons are quasireal implies that $\psi \not\to \gamma 1^{++}$; yet $f_1(1285)$ is seen at a rate comparable[4] to the prominent (QCD allowed) $\psi \to \gamma 2^{++}$. (c) The $f_2(1270, 1525,1720)$ are each seen in $\psi \to \gamma 2^{++}$ and the ratios of their helicity amplitudes ($y \equiv A_2/A_0$; $x \equiv A_1/A_0$) have been measured. It is tantalizing that the x,y for the gluonic candidate $\theta/f_2(1720)$ ($x \approx -1$, $y \approx -1$) differ from the values found[5] for the $q\bar{q}$ states $f_2(1270)$ and $f_2(1525)$ (typically $x \approx 1$, $y \approx 0$) which suggests that the $\theta/f_2(1720)$ is indeed constitutionally different from these $q\bar{q}$ states. Unfortunately it has not been possible to make stronger statements because the measured values of x,y for each of these mesons are many standard deviations away from those predicted in QCD.[6]

This puzzle has been recognized, and unresolved, for over a decade.[7-9] The inclusion of virtual gluons[9] in the intermediate state may resolve problem (b) but makes no measurable impact on (c). The main purpose of this Letter is to propose a resolution that reproduces the data for $f_2(1270,1525)$ rather well and accommodates the rather different structure of the $\theta/f_2(1720)$. A by-product of our work is that the suppression of $\psi \to \gamma 0^{++}$ may also be understood.[10]

In perturbation theory there are two topologies—one where the two gluons are juxtaposed, denoted by A^C, and the other where the photon is emitted between the two gluons, denoted by A^H [Figs. 1(a) and 1(b)]. In perturbative QCD (PQCD) at tree level with effectively unconfined quarks and gluons these diagrams must be added (as in Refs. 6 and 9); however, in the real world of confined colored fields these two contributions have rather distinct interpretations and receive different nonperturbative contributions.

The application of the PQCD results to the physical bound states (quark model) involves the implicit assumptions that nonperturbative physics does not change the helicity ratios in each individual topology and also that it preserves the relative importance of the two topologies. The latter assumption, at least, is almost certainly un-

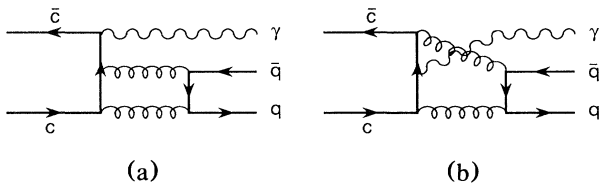

FIG. 1. Two kinds of diagrams for the process $\psi \to \gamma gg \to \gamma M$. (a) Two gluons are juxtaposed, and (b) the photon is emitted between the two gluons.

justified: The charmonium system is well described as $c\bar{c}$ states with little evidence for $c\bar{c}g$ or a higher component in Fock space, yet the topology A^H contains no time ordering where at the instant of γ emission there is a $c\bar{c}$ system alone (contrast to A^C which does include a radiative transition between $c\bar{c}$ states).

We suggest that the empirical failure of Ref. 6 is due to this restrictive assumption that A^C and A^H be treated on an equal footing. We pursue this possibility here by considering the individual topologies separately, illustrating how the original PQCD calculation is broken into the two components and showing that the phenomenological consequences in the quark model are quite different for each topology, where the helicity structure can be determined by the photon transition operator. We shall see that if Fig. 1(b) (A^H) is suppressed, the data for $f_2(1270,1525)$ may be fitted, which is in line with the remarks on $c\bar{c}$ dominance above. However, by contrast, if Fig. 1(b) is dominant, a rather different helicity structure emerges, similar to that for $\theta/f_2(1729)$ empirically. We now substantiate these remarks and consider their implications.

Following the procedure of Krammer,[6] the amplitudes to produce a meson of spin J and spin projection λ along the ψ-γ axis via quasireal gluons $g_\pm$ polarized $\pm$ are determined by

$$A_\lambda \propto \int d\Omega \{A(\psi \to \gamma g_+ g_-)(\theta) d^J_{2\lambda}(\theta) A(g_+ g_- \to M) + A(\psi \to \gamma g_+ g_+)(\theta) d^J_{0\lambda}(\theta) A(g_+ g_+ \to M)\}, \tag{1}$$

$Z \equiv (M_\psi^2 + M_T^2)/(M_\psi^2 - M_T^2)$, and θ is the angle between the momentum of photon and gluons in the rest frame of M_T. Define

$$I(Z,\lambda) \equiv \int \frac{d\Omega (\sin\theta)^{4-2\lambda}(1-\cos\theta)^{2\lambda}}{Z^2 - \cos^2\theta}, \tag{2}$$

and in the approximation that $A(g_+ g_+ \to M) = 0$ for the quasireal gluons coupled to the tensor meson ($J=2$) state,[6,11,12] we find

$$A_2 \propto kM_T I(Z,2), \quad A_1 \propto 2\sqrt{2} kM_\psi I(Z,1), \quad A_0 \propto \sqrt{6}(kM_\psi^2/M_T) I(Z,0), \tag{3}$$

the ratios of which reproduce the results of Krammer,[6] and bear little resemblance to the data.[5] [Relaxing the approximation $A(g_+ g_+ \to M) = 0$ has no effect on A_2:A_0 and so does not resolve the problem.[10]]

But consider now the individual diagrams whose sum was calculated above. We refer to the topology for Fig. 1(a) as A^C, for Fig. 1(b) as A^H, and the total $A^T = A^C + A^H$ is given by Eq. (3). The breakdown is

	A^C	A^H
A_2	0	$kM_T D(Z,2)$
A_1	$\frac{1}{\sqrt{2}} \frac{E_\psi}{M_\psi} k^2 D(Z,1)$	$\frac{1}{\sqrt{2}} \left(kM_\psi - \frac{k^2 E_\psi}{M_\psi} \right) D(Z,1)$
A_0	$\frac{2}{\sqrt{6}} \frac{E_\psi}{M_T} k^2 D(Z,0)$	$\frac{1}{\sqrt{6}} \frac{M_\psi}{M_T} \left(kM_\psi - \frac{2k^2 E_\psi}{M_\psi} \right) D(Z,0)$

(4)

where $D(Z,\lambda) \equiv Z^2 I(Z,\lambda)/\lim_{Z^2 \to \infty} Z^2 I(Z,\lambda)$ is approximately independent of λ in the kinematic region of interest here. So one has

$$\begin{aligned} &y = 0, \quad x = \frac{\sqrt{3}}{2} \frac{M_T}{M_\psi}, \text{ for } A^C; \\ &y = \sqrt{6} \frac{1}{(1 - 2k^2/M_T^2)}, \\ &x = \sqrt{3} \frac{M_T}{M_\psi} \frac{M_T E_\psi - k^2}{M_T^2 - 2k^2}, \text{ for } A^H. \end{aligned} \tag{5}$$

The results for A^C ($y=0$, $x>0$) and A^H ($y<0$, $x<0$) are very different and agree qualitatively with the data for $f_2(1270,1525)$ (A^C: $x_{\text{expt}} \approx 0.9$, $y_{\text{expt}} \approx 0$) and $\theta/f_2(1720)$ (A^H: $x_{\text{expt}} \approx -1.0$, $y_{\text{expt}} \approx -0.6$).

In order to help understand better the physical principle underlying these results we study the radiative transition in the quark model by analogy with Ref. 11 and compare with the perturbative results for A^C and A^H above.

The helicity structure is determined by the matrix elements $\langle T|\mathbf{J}\cdot\boldsymbol{\epsilon}|V\rangle$, where the electromagnetic current $\mathbf{J}$ has the general form[11,13,14]

$$J_+ = AL_+ + BS_+ + CS_z L_+, \tag{6}$$

and V is the real initial vector-meson state. The helicity amplitudes are then

$$A_2 : A_1 : A_0 = \sqrt{6}(A+C) : \sqrt{3}(A+B) : A + 2B - C. \tag{7}$$

If the states $|V\rangle$ and $|T\rangle$ are $c\bar{c}$ states, the nonrelativistic forms of A, B, and C should be

$$A = 4\sqrt{\pi/k}\, \mu \langle T|qe^{-i\mathbf{k}\cdot\mathbf{r}} p_+|V\rangle, \tag{8}$$

$$B = 4\sqrt{\pi/k}\, \mu k \langle T|qe^{-i\mathbf{k}\cdot\mathbf{r}}|V\rangle, \tag{9}$$

and

$$C=0. \tag{10}$$

where the valence quark has magnetic moment $\mu=e/2m_q$, charge q, and $p_+=-(1/\sqrt{2})(p_x+ip_y)$ probes the transverse momentum p_t of confined charmed quarks and generates the electric dipole ($E1$) transition for $\mathbf{k}\to 0$. In general, $B/A\sim\mathbf{k}^2/p_t^2$ and taking the limit $\mathbf{k}\to 0$, we have $B=C=0$ and recover $E1$ dominance [as in $\psi'\to\gamma\chi$ (Refs. 14 and 15)]. But the spin-flip term becomes increasingly important as $\mathbf{k}^2$ grows [this is akin to the behavior seen in $\gamma(k^2)N\to N^*$,[16] where $\mathbf{k}^2$ varies as k^2 varies; in $\psi\to\gamma(k)X$ it is the varying M_T^2 that causes $\mathbf{k}$ to change]. For $\psi\to ggg\to\gamma M$, $B/A\sim\mathbf{k}^2/p_t^2\gg 1$ in the kinematic region with $M_T\sim 1$–2 GeV, which implies $A/B\approx C=0$ and hence $y=0$, $x=\sqrt{3}/2$ (see also Ref. 7). As a specific example we can use a harmonic-oscillator quark model for which

$$y=\sqrt{6}\frac{1}{1+2k^2/\beta_{\rm SHO}^2},\quad x=\sqrt{3}\frac{1+k^2/\beta_{\rm SHO}^2}{1+2k^2/\beta_{\rm SHO}^2}, \tag{11}$$

where $\beta_{\rm SHO}^2=0.245$ GeV^2 (Ref. 17) is the momentum scale (and measure of $\langle p_t^2\rangle$) determined by the quark mass and the oscillator strength. For $f_2(1270)$ [$f_2(1525)$], this gives $x=0.92$ [0.94] and $y=0.17$ [0.20].

In analogy to Ref. 11, one can factorize the amplitude $A(\psi\to\gamma g_+g_-)$ in Eq. (1) into $O_\gamma\otimes O_{gg}$ (the photon transition operator O_γ and two-gluon transition operator O_{gg}), and develop the connection between the PQCD and the quark-model approach.[10] So, the process $\psi\to\gamma g_+g_-$ can be treated sequentially: (i) $\psi\to\gamma T$ which is determined by the photon transition operator O_γ; (ii) $T\to gg$ determined by O_{gg}. In this particular model the nonperturbative effects are subsumed in the intermediate tensor state T, while the operators O_γ and O_{gg} remain unchanged; thus Eq. (1) becomes

$$A_\lambda\propto\langle T_\lambda|O_\gamma|V_{\lambda-1}\rangle|A(g_+g_-\to M)|^2I(Z,\lambda), \tag{12}$$

where $A(g_+g_-\to M)$ is the transition amplitude for $T\to gg$. The photon transition operator O_γ is[10]

$$O_\gamma=\begin{cases}\boldsymbol{\sigma}\cdot(\boldsymbol{\epsilon}\times\mathbf{k})\mathbf{k}\cdot\mathbf{p}, & \text{for } A^C,\\ M_T^2\mathbf{p}\cdot\boldsymbol{\epsilon}-i\boldsymbol{\sigma}\cdot(\boldsymbol{\epsilon}\times\mathbf{k})\mathbf{k}\cdot\mathbf{p}, & \text{for } A^H,\end{cases} \tag{13}$$

where $\boldsymbol{\epsilon}$ and $\mathbf{k}$ are the polarization vector and the momentum of the photon, $\mathbf{p}$ is the constituent internal momentum, and M_T is the mass of the tensor meson.

The absence of a $\mathbf{p}\cdot\boldsymbol{\epsilon}$ contribution in A^C follows because of Krammer's assumption that the internal transverse momentum $p_t=0$. Comparing Eq. (13) with Eq. (6) shows that only $B\neq 0$ for A^C, which leads to the Clebsch-Gordan coefficient $\sqrt{3}/2$ in x (Ref. 7) and $y=0$ in Eq. (5). Similarly, one can establish the connection between the expressions of the quark model [Eq. (7)] and the PQCD [Eq. (5)] for A^H. In this case there is a $\mathbf{p}\cdot\boldsymbol{\epsilon}$ contribution whose origin is in transverse momentum generated by gluon radiation. Comparison with Eq. (6) shows that $B/A=-k^2/M_T^2$ and $C=0$, so one has

$$y=\sqrt{6}\frac{1}{1-2k^2/M_T^2},\quad x=\sqrt{3}\frac{1-k^2/M_T^2}{1-2k^2/M_T^2} \tag{14}$$

(the difference between PQCD [Eq. (5)] and the quark model [Eqs. (11) and (14)] is due to the neglect of the longitudinal recoil effects in the quark model).

The crucial distinction between the dynamics of A^C and A^H is the role of the transverse momentum of the $c\bar{c}$. If we ignore multiquark components in the wave function, the topology for Fig. 1(a) is equivalent to a transition between the $\psi(c\bar{c})$ and a virtual state $\chi(c\bar{c})$ [or $\psi(c\bar{c}g)$,$\chi(c\bar{c}g)$ states] where the c or $\bar{c}$ that radiated the photon in the initial state has *limited transverse momentum* and hence $y\approx 0$. The topology for Fig. 1(b) corresponds to transitions between hybrid components $\psi(c\bar{c}g)$ and $\chi(c\bar{c}g)$ where the net spin of the $c\bar{c}$ differs from that of $\psi(c\bar{c})$ or $\chi(c\bar{c})$ and the quark or antiquark *can have relatively large* p_t.

If the $\psi(c\bar{c})$ wave function has limited p_t then the amplitude ratios for $f_2(1270,1525)$ emerge naturally. To the extent that they are driven by the A^C topology, they need be no test of QCD at all because if there were any $c\bar{c}$ component in the Fock state of the final-state meson, the dominant contribution would be production through Fig. 1(a). Alternatively, if the $c\bar{c}g$ component in the ψ is small (as suggested by the successful description of charmonium in potential models) one again anticipates that Fig. 1(a) will dominate unless there is some favoring of $c\bar{c}g$ coupling to the final state.

The emerging data on the $\theta(1720)$ show rather different behavior, in particular, $y\neq 0$, requiring $p_t\neq 0$ in the initial state. Within PQCD this is generated by gluon radiation [Fig. 1(b)], which also causes $y<0$. In the nonrelativistic quark model of charmonium, where gluons play no explicit role, $x>0$, $y\geq 0$ [e.g., Eq. (11) and Ref. 10]. If the data on the θ production $x<0$, $y<0$ survive, then PQCD would suggest that this is intimately connected with gluons playing an explicit role in the $c\bar{c}$ bound state; in turn, if gluons are active in the bound state the failure of the $c\bar{c}$ quark model (to accommodate negative x,y) would also be explained. If these speculations are substantial, prominence of the θ in ψ radiative decays and its production via a minor $c\bar{c}g$ part of the ψ wave function would suggest that glue plays a major role in the θ production.

One natural extension of our work is to $\psi\to\gamma 1^{(++)}$ which goes beyond the restriction to quasireal gluons in the intermediate state. Such a program is in progress.

This work was supported in part by the State of Tennessee Science Alliance Center and the U.S. Department of Energy under Contract No. DE-AS05-76ER0-4936.

[1] W. Dunwoodie, in Proceedings of the Workshop on Hadron

Mass Spectrum ("Hadron 90"), St. Goar, Germany, 3–6 October 1990 (to be published); S. Godfrey, *ibid.*; F. Close, in *The Storrs Meeting,* Proceedings of the 1988 Meeting of the Division of Particles and Fields of the APS, Storrs, CT, 1988, edited by K. Haller *et al.* (World Scientific, Singapore, 1989), p. 432.

[2]J. Weinstein, in Proceedings of the Workshop on Hadron Mass Spectrum (Ref. 1); J. Weinstein and N. Isgur, Phys. Rev. D **27**, 588 (1983); R. L. Jaffe and F. E. Low, Phys. Rev. D **19**, 2105 (1979); D. Morgan and M. Pennington, Rutherford Laboratory Report No. RAL-90-030 (to be published).

[3]F. Close, in Proceedings of the Workshop on Hadron Mass Spectrum (Ref. 1), Conference summary talk, and references therein.

[4]W. Lockman, in Proceedings of the Workshop on Hadron Mass Spectrum (Ref. 1); M. Burchell, *ibid.*; DM2 Collaboration, L. Stanco *et al.*, *ibid.*

[5]C. Edwards *et al.*, Phys. Rev. D **25**, 3065 (1982); D. Hitlin, in *Glueballs, Hybrids and Exotic Hadrons,* edited by S. U. Chung, AIP Conf. Proc. No. 185 (AIP, New York, 1988); L. Chen, in Proceedings of the Workshop on Hadron Mass Spectrum (Ref. 1).

[6]M. Krammer, Phys. Lett. **74B**, 361 (1978).

[7]F. E. Close, Phys. Rev. D **27**, 311 (1983).

[8]D. V. Bugg, J. Phys. G **13**, 4169 (1987); B. F. L. Ward, Phys. Rev. D **33**, 1900 (1986).

[9]J. Korner, J. Kuhn, M. Krammer, and H. Schneider, Nucl. Phys. **B229**, 115 (1983).

[10]F. E. Close and Z. P. Li, Rutherford Appleton Laboratory–University of Tennessee at Knoxville Report No. RAL-91-039, UTK-91-003 (to be published).

[11]Z. P. Li, F. E. Close, and T. Barnes, Phys. Rev. D **43**, 2161 (1991).

[12]M. Krammer and H. Kraseman, Phys. Lett. **73B**, 58 (1978).

[13]F. J. Gilman and I. Karliner, Phys. Rev. D **10**, 2194 (1974); J. Babcock and J. Rosner, Phys. Rev. D **14**, 1286 (1976).

[14]F. E. Close, *Introduction to Quarks and Partons* (Academic, New York, 1979), p. 369.

[15]J. D. Jackson, in *Proceedings of the Summer Institute on Particle Physics, Stanford,* edited by M. Zipf (SLAC Report No. 198, 1976).

[16]F. E. Close and F. J. Gilman, Phys. Lett. **38B**, 541 (1972); F. E. Close, F. J. Gilman, and I. Karliner, Phys. Rev. D **6**, 2533 (1972).

[17]C. Hayne and N. Isgur, Phys. Rev. D **25**, 1944 (1982).